JOURNAL OF THERMOPHYSICS AND HEAT TRANSFER
Vol. 22, No. 3, July–September 2008

Feasibility Study of Cooling Enhancement with Porous Metal Inserts

Kun Yuan,* Yan Ji,* and J. N. Chung†
University of Florida,
Gainesville, Florida 32611

DOI: 10.2514/1.33910

In general, for power and propulsion components, the bottleneck of their performance advancement is usually associated with the heat-dissipation capability. For example, rocket propulsion has been used in many different aspects of space travel and military tasks. With the higher demand today for longer-lasting and farther travel and with the extreme temperatures that these elements experience, a breakthrough technology is needed in the cooling of these thrust chambers. In this paper, the idea of using porous metallic foams is examined for their cooling-enhancement capabilities. The goal is to provide more cooling without creating additional pressure drops in the coolant passage. An experimental system was used to investigate the heat transfer enhancement and pressure drop in an annular channel filled with nickel or copper foams. The coolant used was compressed air at 1378 kPa. Constant-heat-flux heaters placed inside the inner tube of the annulus were used to simulate the heat source. Then the experiment was performed under steady state. For both the copper- and nickel-foam-filled annular channels, the heat transfer enhancement was found to be on the order of 20 times over the annular channel without porous insert for the same Darcy velocities. The pressure drop per unit channel length of the foam-filled channel is at least 2 orders of magnitude larger than that in the annular channel without porous insert; therefore, at equal pumping powers in the range of 10 to 100 W, the heat transfer enhancement of an annular metal-foam-filled channel over an annular channel without porous insert is around 3 to 4 times. When assessing the feasibility of applying the metal-foam-filled cooling channel for liquid-fueled rocket engines, we found that heat transfer enhancement ranges between 105 to 150% for equal pressure drops and mass flow rates.

Nomenclature

A_s	=	inner tube heated surface, m^2
c_p	=	specific heat, $J/kg \cdot K$
d_i	=	inner diameter of the annulus, m
d_o	=	outer diameter of the annulus, m
f	=	friction factor
h	=	heat transfer coefficient, $W/m^2 \cdot K$
k	=	thermal conductivity, $W/m \cdot K$
m	=	mass flow rate, kg/s
Nu	=	Nusselt number
Pe	=	Peclet number
Pr	=	Prandtl number
$\dot{q}$	=	heat transfer rate, W
Q	=	volumetric flow rate, m^3/s
Re	=	Reynolds number
R_{th}	=	heat transfer resistance, K/W
$T_{a,\text{inlet}}$	=	inlet air temperature, K
$T_{a,\text{outlet}}$	=	outlet air temperature, K
T_b	=	bulk temperature, K
T_s	=	surface temperature, K
u	=	velocity, m/s
$\dot{W}$	=	pumping power, W
ΔT	=	temperature difference, K
ε	=	porosity
μ	=	viscosity, $N \cdot s/m^2$
ρ	=	density, kg/m^3

Presented as Paper 4128 at the 41st AIAA Joint Propulsion Conference, Phoenix, AZ; received 6 August 2007; revision received 17 January 2008; accepted for publication 11 February 2008. Copyright © 2008 by the American Institute of Aeronautics and Astronautics, Inc. All rights reserved. Copies of this paper may be made for personal or internal use, on condition that the copier pay the $10.00 per-copy fee to the Copyright Clearance Center, Inc., 222 Rosewood Drive, Danvers, MA 01923; include the code 0887-8722/08 $10.00 in correspondence with the CCC.

*Graduate Student, Department of Mechanical and Aerospace Engineering, P.O. Box 116300.

†Professor, Department of Mechanical and Aerospace Engineering, P.O. Box 116300. Member AIAA.

I. Introduction

THE structure of a rocket engine thrust chamber is quite complex and has been studied extensively in the past. It is in the form of a converging–diverging nozzle. This shape provides for the maximum thrust and engine performance needed by the propulsion system. The successful design has had an ongoing struggle with the amount of cooling necessary for the thrust-chamber element. The skin of the nozzle has to be able to withstand high temperatures and high pressures and has to be lightweight. To achieve very high thrusts, the combustion of the oxidizer and the fuel must be very intense. Therefore, the gases that escape through the nozzle after combustion are extremely hot (~2800 K). For many years, the idea of a cooling jacket has been used to surround the outside of this nozzle and the chamber. The purpose for this cooling jacket is to cool the inner walls of the combustion chamber and nozzle regions, which can help in many ways. First, the parts surrounding the outside of this nozzle will not experience as much of the heat from the combustion. Second, the materials of the nozzle itself will be at a much cooler temperature range, thus increasing its life expectancy. Third, the use of lighter materials will help with the overall weight requirement of the system.

Recently, even with new advances in high-temperature materials, the bottleneck of thrust increases for large liquid-propellant rocket engines is still controlled by the cooling capacity around the combustion chamber. Especially at the exhaust nozzle area, where the heat flux level peaks, breakthrough cooling technology is needed to meet the challenge. In the past, active cooling methods have been applied to the rocket engines. Active, or regenerative, cooling involves transferring the heat from the chamber to the propellant, which acts as a coolant, before combustion. These active cooling devices have been in the form of conventional tube-wall heat exchangers, in which cooling fluids flowing through open tubes, milled channels, and coils.

Based on a survey of the literature, we found that a potential breakthrough in rocket engine cooling, which would result in

possible orders-of-magnitude improvement in engine performance, could come from filling the coolant passages with a high-conductivity porous medium or open-cell foam. Koh and Colony [1] and Koh and Stevens [2] investigated the enhancement of heat transfer for forced convection in a channel filled with a high-thermal-conductivity porous medium. In their theoretical study, Koh and Colony [1] found that for a fixed-wall-temperature case, the heat transfer rate increased by 3 times. For a constant-heat-flux case, the wall temperature and the temperature difference between the wall and the coolant can be drastically reduced. Koh and Stevens [2] performed experimental work to verify the numerical results of Koh and Colony [1]. Koh and Stevens [2] used a stainless steel cylindrical annulus (3.8-cm i.d. and 5.1-cm o.d.) with a length of 8 in. to experiment with heat transfer enhancement by a porous filler. The annulus was filled with peen shot (steel particles) with diameters of from 0.2 to 0.25 cm. Nitrogen gas was the coolant that flowed through the annulus. They found that the heat flux increased from 1.5 to 3.3 W/m^2 for a constant-wall-temperature case and the wall temperature dropped from 788 to 177°C for the constant-heat-flux case.

Hunt and Tien [3] used foamlike material and fibrous media to enhance forced convection for potential application to electronics cooling. Their results showed that a factor of 2 to 4 times the enhancement is achievable, compared with laminar slug flow in a duct. Maiorov et al. [4] empirically found that the heat transfer rates in channels with a high-thermal-conductivity filler, compared with empty channels, reached a factor of 25–40 enhancement for water and 200–400 for nitrogen gas. Bartlett and Viskanta [5] developed a mathematical model to predict the enhancement by high-thermal-conductivity porous media in forced convection duct flows. They concluded that a 5–30 times increase in heat transfer is feasible for most engineering conditions. It is believed that the enhancement is mainly due to the microturbulent mixing in the pores and super heat transfer through high-thermal-conductivity porous structure. The enhancement is also due to the increased surface area.

Kuzay et al. [6] reported liquid-nitrogen convective heat transfer enhancement with copper matrix inserts in tubes. They claimed that the insertion of porous copper mesh into plain tubes enhances the heat transfer quite extensively with a single-phase coolant. However, in boiling, with tubes in which the porous insert is brazed to the tube wall for the best thermal contact, the heat enhancement was on the order of fourfold relative to a plain tube. They concluded that porous matrix inserts offer a significant advantage in cooling, providing a jitter-free operation and a much higher effective heat transfer, at grossly reduced flow rates relative to plain tubes. More recently, as a result of materials manufacturing breakthroughs, very-high-porosity (greater than 90%) open-cell metal foams became available that gave rise to a strong interest in the applications of these metal foams to heat transfer enhancement. Boomsma et al. [7] used an open-cell aluminum-alloy metal foam measuring $40 \times 40 \times 2$ mm as a compact heat exchanger to evaluate the electronic cooling potential. With liquid water as the working fluid, they found that the heat exchanger generated resistances that are 2 to 3 times lower than those of the open-channel heat exchanger and required the same pumping power. Additionally, several experimental investigations [8–11] have provided heat transfer and pressure-drop information for channels and pipes with metal-foam inserts. At the same time, modeling and analysis efforts [12–14] were reported for metal-foam-induced increases in heat transfer and pressure drop.

Based on discoveries by the preceding researchers, we hope that breakthrough advancement in the development of new technologies for rocket engine cooling is within our reach. The porous or open-cell foam layer has the potential to offer orders-of-magnitude improvement in cooling capacity. The objective of this paper is to investigate the feasibility of using metal foams to enhance cooling for the thrust chamber. It is noted that the cooling-enhancement technology addressed here can be applied to many other components in power and propulsion systems that rely on more cooling to improve performance. This paper documents a systematic study on the preliminary development of a high-performance cooling system for rocket engines. The key component of the cooler is based on high-thermal-conductivity porous medium or open-cell foam-filled channels with forced convection of propellant fluids.

II. Experimental System

The experimental system consists of a needle valve, a flow meter, inlet region, test section, outlet region, and data acquisition system. Figure 1 shows the schematic of the experimental system.

Consistent compressed air is supplied to the experimental system with a maximum pressure of 1378 kPa. The needle valve is used to regulate the flow rate with a high accuracy. To measure accurate flow rates, three different flow meters are used to cover different flow rate ranges: Omega FL4512 (for flow rates less than 12 liter/s), Omega FL4412 (for flow rates in the range of 12–46 liter/s), and King instrument 7700 (for flow rates in the range of 120–210 liter/s). The inlet region is stainless steel pipes of 91.44-cm length with 4.8-cm o.d. and 4.1-cm i.d.. Three pieces of stainless steel meshes are placed into the inlet region to ensure well-mixed uniform airflow. The outlet region has the same o.d. and i.d. as the inlet region. The length of the outlet region is 20.32 cm.

Two types of test sections are used in the experiment. One is an annulus with either a nickel-alloy or copper metal-foam insert that is brazed to the inner wall, and the other is an annular channel without porous insert with the same dimensions. For the metal-foam test section, the annular metal foam has a 4.1-cm o.d. and a length of 12.7 cm that is brazed on the stainless steel pipes of 2.68-cm o.d. A cartridge heater of 12.7 cm long is inserted into a 12.7-cm-long copper tube and firmly inserted into the test section to provide a constant-heat-flux heating. To minimize the axial heat transfer, the copper tube is coupled with two Teflon tubes of 6.35-cm length at both ends. A 63.5-cm-long copper tube capped at one end is connected to one of the Teflon tube and inserted inside the inlet region. This ensures that the airflow is fully developed before it goes

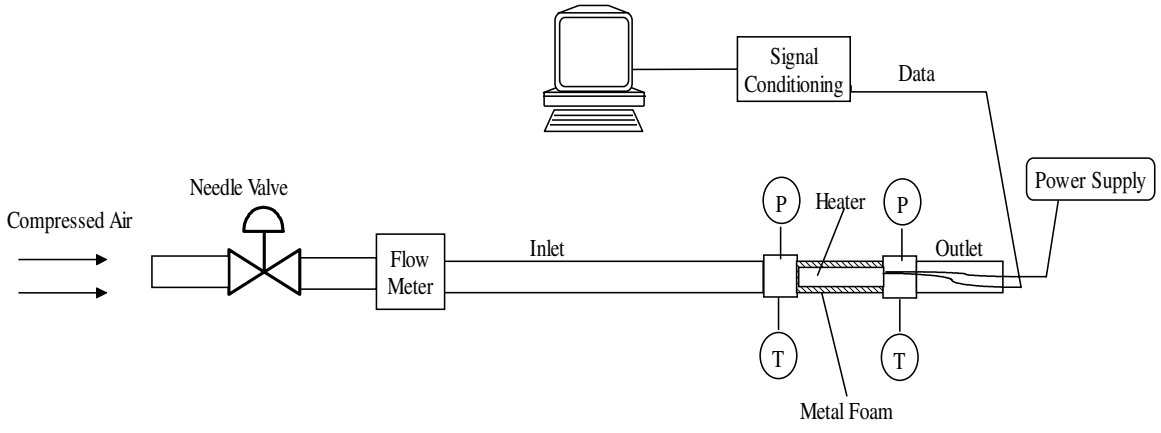

Fig. 1 Sketch of the experimental system.

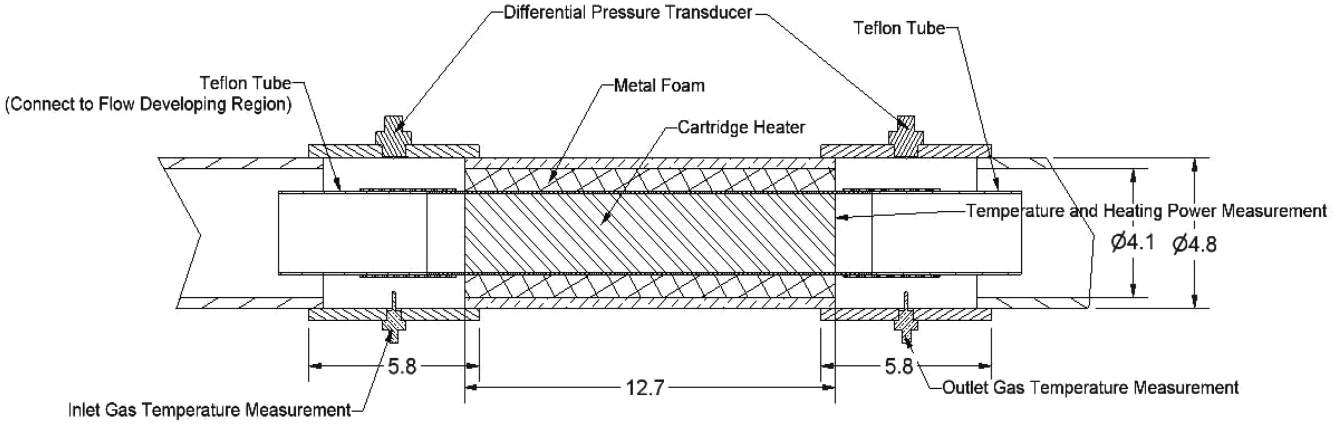

Fig. 2 Sketch of the test section.

into the test section. The outside of the test section is a 12.5-cm-long aluminum pipe. Fiberglass insulation is placed around the aluminum pipe. Figure 2 gives the dimensions of the test section and a detailed view of how the system is assembled. The test section of the annular channel without porous insert has the same dimensions as the metal-foam test section, except that no metal foam is placed on the stainless steel pipe. Therefore, the airflow goes through the annulus between the test section and the aluminum pipe. The test for the annular channel without porous insert is used as a calibration and a basis for comparison to the metal-foam test.

We used both nickel and copper foams. The metal foams were purchased from the Porvair company. The foams have a layered structure, as shown in Fig. 3 for the nickel foam, and the cells have a pentagon shape. We used a cell size of 0.254 cm (0.1 in.) (10 pores per inch, or 10 PPI) approximately. The ligaments have an average thickness of 263 μm. The porosity is 95% and the relative density is therefore 5%. General properties of the foams are provided in Table 1. The brazing of the metal foams onto the wall was performed by the Porvair company with metal foils and pressing under elevated temperatures. The data collected during the experiments were flow rate, pressure, and temperature. The flow rate was adjusted by the needle valve and measured by the flow meter; it remains constant in each test.

An Omega PX203-200G5V pressure transducer of 0.25% full-scale accuracy is used to measure the inlet pressure at the inlet region. Accurate measurement of the pressure-loss characteristic of metal foam is very important. So a differential pressure transducer (Validyne DP1540N1S4A) with changeable diaphragms is used to measure the pressure drop just before and after the test section. Two diaphragms are used in the test (Validyne 3-22 and 3-40); both diaphragms have a 0.25% full-scale accuracy and can be overpressured up to 200%. The pressure range of Validyne 3-22 is 0–1.4 kPa and the pressure range of Validyne 3-40 is 0–86 kPa. Each time the diaphragm is changed, the pressure transducer is recalibrated. The pressure transducer is powered by a Validyne DP16A1A demodulator. In total, 16 thermocouples are used at different downstream locations. Five type-K thermocouples with fiberglass insulation are used to measure the outside wall temperatures of the test section. The locations of these five thermocouples are indicated in Fig. 4. Both the airflow inlet and outlet temperatures are measured with three type-T thermocouples. The inlet and outlet air temperature is then the average of these three temperatures. The average of these two temperatures is used as the balk temperature of the airflow. The difference of these two temperatures is used in the energy-balance equation to calculate the heat carried by the airflow. Another four type-T thermocouples are placed at different locations before and after the test section, which are used to calculate the axial heat leakage. The outside wall temperature of the test section is also measured and used to calculate the heat loss to the environment. All the thermocouples are connected to a 16-channel screw terminal board and then to an A/D board (Measurement Computing PCI-DAS-TC). Both A/D boards are plugged into the PCI (peripheral component interconnect) slot of a computer. A LabVIEW program is applied to control both the pressure and the temperature acquisition.

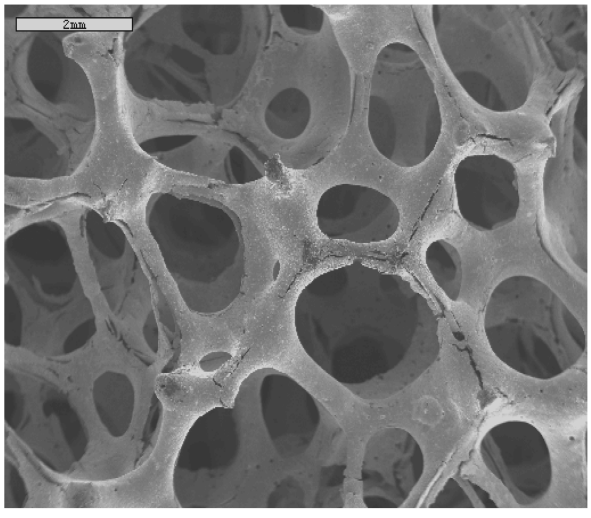

Fig. 3 Scanning electron microscope photograph of the nickel foam.

III. Experimental Procedure and Data Reduction

First, the needle valve is opened to the maximum opening and the cartridge heater is turned on. The compressed air passes through the experimental system with the maximum flow rate. The steady state is considered to be attained when the temperatures indicated by the thermocouples do not vary more than $\pm 0.3^{\circ}$C within 1 min. An initial period of approximately 0.5 h is usually required before the system can reach steady-state condition. After reaching steady state, the needle valve is adjusted to decrease the flow rate and wait for the system to reach the next steady state.

The heat transfer rate to the airflow is defined by the energy balance:

$$\dot{q} = \dot{m} c_p (T_{a,\text{outlet}} - T_{a,\text{inlet}}) \tag{1}$$

where $T_{a,\text{outlet}}$ and $T_{a,\text{inlet}}$ are the outlet and inlet air temperatures, respectively, and c_p is the specific heat under a constant pressure. The bulk temperature is defined as

Table 1 Properties of copper and nickel foams

Foam material	Density, kg/m^3	Thermal conductivity, W/m · K	Specific heat, J/kg · K
Copper	8933	396	397
Nickel	8366	485	14

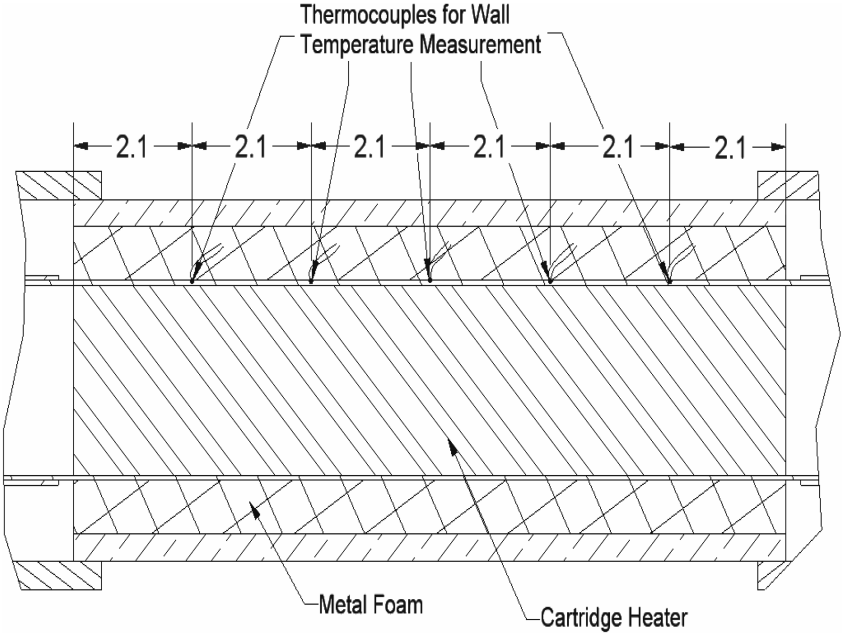

Fig. 4 Locations of thermocouples in the test section.

$$T_b = (T_{a,\text{outlet}} + T_{a,\text{inlet}})/2 \tag{2}$$

Local heat transfer coefficient is defined as

$$h = \dot{q}/A_s(T_s - T_b) \tag{3}$$

where A_s is the total inner tube heated surface area and T_s is the mean of the surface temperatures measured by the type-K thermocouples. The Reynolds number is defined as

$$Re = \frac{u\rho(d_o - d_i)}{\mu} \tag{4}$$

where u is the Darcy velocity (average velocity of the annular channel without porous insert or average velocity before entering the metal foam), and d_o and d_i are the outer and inner diameter of the annulus, respectively. The Nusselt number is defined as

$$Nu = \frac{h(d_o - d_i)}{k} \tag{5}$$

In Eq. (5) k is the thermal conductivity of the working fluid air.

The uncertainties for the measured and calculated values are as follows: ±0.38 kPa for pressure, ±0.5°C for temperature, ±4% for mass flow rate, ±8% for the Reynolds number, ±8% for the heat transfer coefficient, and ±8% for the Nusselt number.

IV. Experimental Results and Discussion

A. Test Results for the Annular Channel Without Porous Insert

The test for the annular channel without porous insert was performed with different flow rates: namely, 30.4, 26.9, 22.9, 20.9, 19.0, 17.1, 14.3, and 11.4 l/s. The corresponding Reynolds number range is 13,291–35,331, which means that the flow is turbulent. The pressure drops measured by the differential pressure transducers are averaged during the steady state in each test. Figure 5 shows the pressure-drop curves for various Reynolds numbers. As expected, the pressure loss increases with increasing Reynolds number. For calibration purposes, the measured pressure drops are also compared with an empirical correlation. The predicted pressure drop is calculated from the friction factor, which is defined as

$$f = \frac{(\Delta p/\Delta L)d_h}{(0.5\rho u^2)} \tag{6}$$

The empirical correlation for the turbulent friction factor is the universal law of friction for smooth pipes given by Prandtl [15], as follows:

$$\frac{1}{f^{0.5}} = 2.0\log(Re_D f^{0.5}) - 0.8 \tag{7}$$

The differences between the current experimental results and those from the empirical correlation as seen in Fig. 4 are within reasonable uncertainties.

For the test for the annular channel without porous insert, the power output of the cartridge heater is 250 ± 5 W. The heat transferred to the airflow is calculated by the energy balance with Eq. (1). It is found that about 55–70% of the heat released from the heater is carried by the airflow, depending on the flow rate. The rest of the heat is lost by conduction and radiation. Figure 6 illustrates the temperature curves of $T_{a,\text{inlet}}$ and $T_{a,\text{outlet}}$ and the five surface temperatures of the stainless steel pipe. It is found that the temperature distributions are more even inside the heated surface for higher flow rates. The temperature difference between the airflow and the heated surface decreases with the increasing flow rate, which implies a higher heat transfer coefficient at a higher Reynolds number.

The Nusselt number as a function of the Reynolds number was evaluated based on the definition given in Eq. (5). Figure 6 shows the

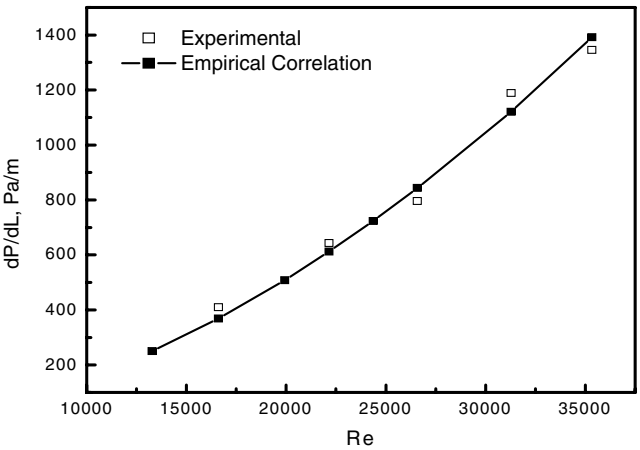

Fig. 5 Pressure-drop curves for tests of the annular channel without porous insert.

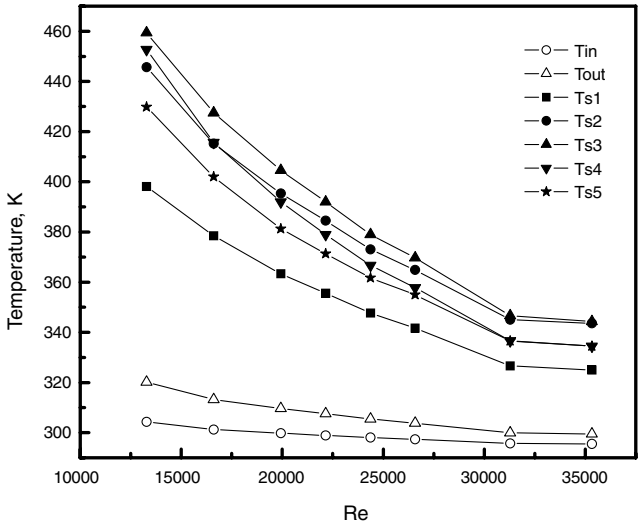

Fig. 6 Temperature curves of the inlet and outlet airflow and the heated surface.

relationship between the Nusselt number and the Reynolds number. It is found that the Nusselt number increases with increasing Reynolds number, because the airstream with a higher flow rate will carry away more heat. An empirical correlation for the turbulent internal gas flow was suggested by Gnielinski [16]:

$$Nu = 0.024(Re^{0.8} - 100)Pr^{0.4}\left[1 + \left(\frac{d}{l}\right)^{2/3}\right]\left(\frac{T_b}{T_s}\right)^{0.45} \quad (8)$$

where Pr is the Prandtl number of the airflow, and d and l are parameters to correct for entrance effects. We use the average of the five surface temperatures given by the type-K thermocouples for T_s. The calculated empirical values for the Nusselt number are shown in Fig. 7. It is found that the experimental results agree well with the empirical results. The two curves cross each other at the Reynolds number around 3200, which is basically due to uncertainties from the natural scattering of the experimental measurements.

B. Test Results for the Foam-Filled Case

The measured pressure-drop and heat transfer data for the foam-filled annular channel are presented with those of the annular channel without porous insert, for the purpose of comparison. The pressure drop per unit channel length vs the Darcy velocity is plotted in Fig. 8.

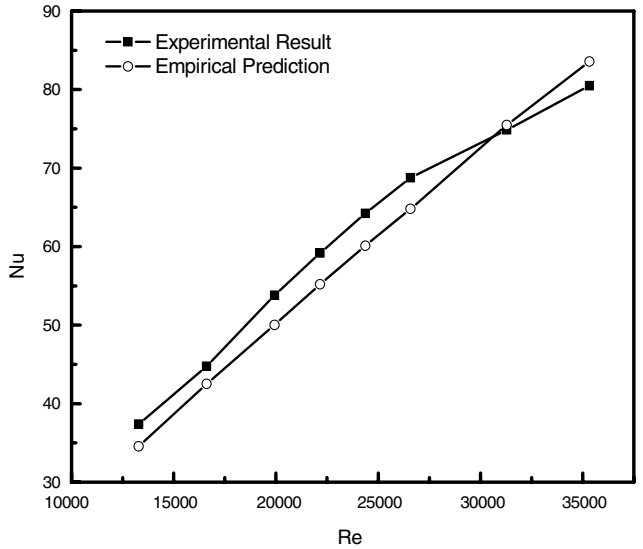

Fig. 7 Heat transfer coefficient for tests of the annular channel without porous insert.

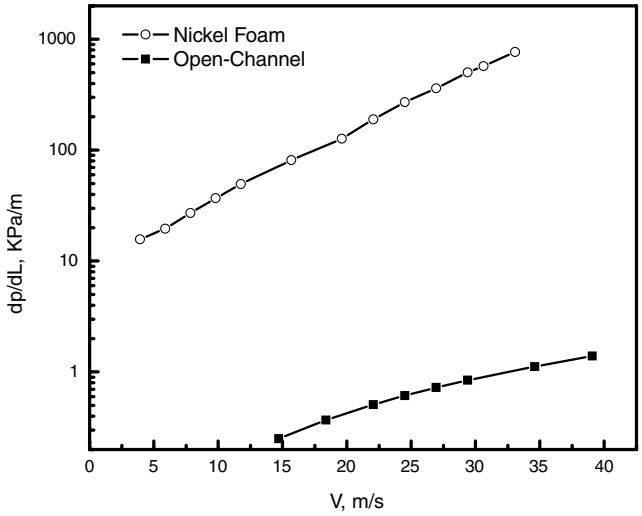

Fig. 8 Measured pressure drop per unit channel length for both annular channel with no porous insert and foam-filled annular channel.

It is clear that the pressure drops for the foam-filled channel are generally two or more orders of magnitude higher than those for the annular channel without porous insert. Both curves are relatively linear on the semilog plot. The main reason for the substantially elevated pressure-drop levels for the foam-filled channel is the huge surface area per unit volume associated with the structure of the foam, as seen in Fig. 3, that gives rise to the skin-friction loss even though the porosity is very high. Additionally, extra pressure losses are caused by the local contraction and expansion, in addition to vortex shedding behind ligaments.

The most important objective of this research is the understanding and evaluation of the heat transfer enhancement facilitated by the large surface area per unit volume from the microscale ligaments that act as fins. Figure 9 gives the heat transfer coefficient vs the Darcy velocity for both the annular channel without porous insert and the foam-filled cases. It is noted that the heat transfer coefficient curve exhibits two trends for laminar and turbulent flows, respectively. The transition from laminar to turbulent flows takes place around the Darcy velocity of 12 m/s. The enhancement ratio of the heat transfer coefficients is plotted in Fig. 10 for the turbulent flows. It is seen in Fig. 10 that the enhancement ratio ranges between 21 and 25, which is very consistent, barring experimental uncertainties. The enhancement ratio over 20 is higher than many of those reported in the literature. We strongly believe that this higher enhancement ratio is basically due to two physical mechanisms. The first is that the foam

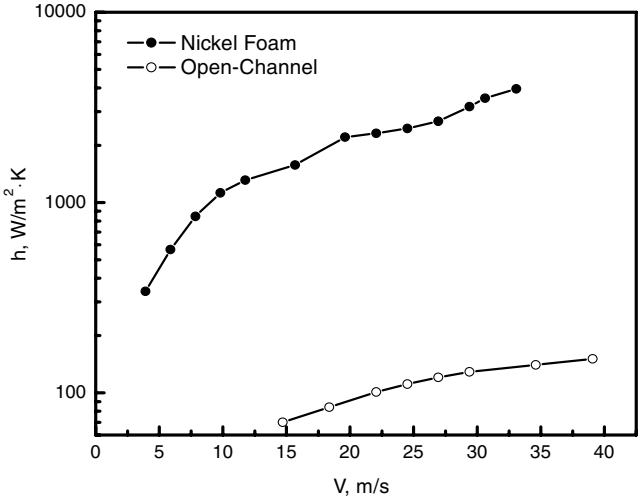

Fig. 9 Measured heat transfer coefficient for both annular channel with no porous insert and foam-filled annular channel.

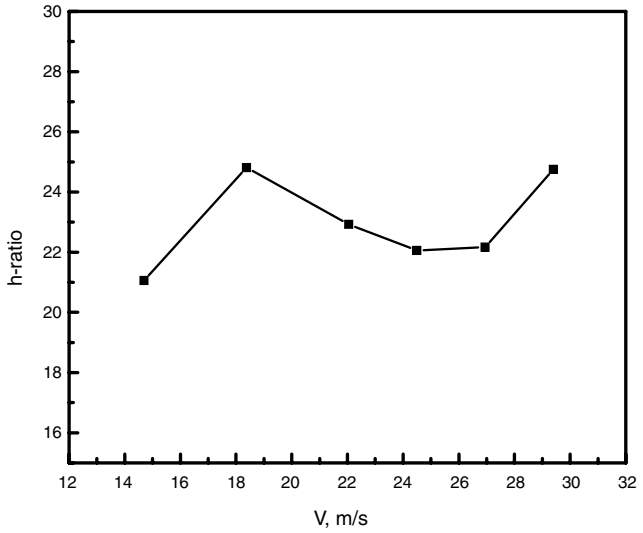

Fig. 10 The ratio of foam-filled channel to the channel with no porous-insert heat transfer coefficients as a function of Darcy velocity.

used in our case is composed of thin-layered ligaments that offer much more surface area per unit volume than common porous media such as granular and fibrous materials. The second reason is that the velocity range applied in our case corresponds to highly turbulent flows, compared with laminar flows in most reported cases [7–9] in the literature.

For the applications to be feasible in liquid-fueled rocket engines, the issue of pressure drop must be weighed with the heat transfer enhancement, because we can see that the penalty is severe from pressure losses. Figure 11 is a plot of the pumping power vs the heat transfer resistance for both the annular channel with no porous insert and the foam-filled annular channel. The pumping power is defined as

$$\dot{W} = \Delta P Q \tag{9}$$

where ΔP is the pressure drop across the test section and Q is the volumetric flow rate. Heat transfer resistance is often used to measure the convective heat transfer effectiveness. It is also the inverse of convection conductance. It is defined as

$$R_{\text{th}} = \frac{\Delta T}{\dot{q}} = \frac{T_s - T_{a,\text{inlet}}}{\dot{m} c_p (T_{a,\text{outlet}} - T_{a,\text{inlet}})} = \frac{1}{hA_s} \tag{10}$$

Based on Fig. 11, at an equal pumping power in the range of 10 to 100 W, the heat transfer enhancement due to the foam is in the range of 3 to 4 times.

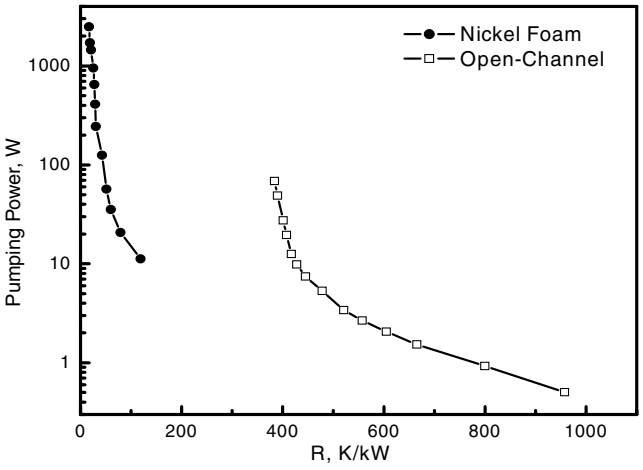

Fig. 11 Pumping power vs heat transfer resistance for both annular channel with no porous insert and foam-filled annular channel.

Table 2 Micro-open-channel and foam-filled channel model requirements

	Micro open channel	Foam channel
Channel width	2 mm	2 mm
Channel height	4 mm	x mm
Pressure drop	A	A
Coolant flow rate	B	B
Heat transfer	$Q1$	$Q2 > Q1$

V. Feasibility for a Rocket Engine Thrust-Chamber Cooling

A. Current Rocket Engine Cooling Channel Design

Most rocket engine thrust-chamber cooling jackets are in the form of either microtubes or milled microchannels [17]. The microscale nature of the cooling channels is intended for achieving high heat transfer coefficients. For a meaningful feasibility study with respect to a thrust-chamber cooling system, we have adopted the typical open-milled microchannel design suggested by Wennerberg et al. [18] as the baseline case for comparison with the foam-filled channel. Two models (foam vs open microchannel) are developed for a head-to-head comparison. The basic requirements for the two models are listed in Table 2.

Figure 12 shows the model schematics for a micro open channel and a foam-filled channel, respectively. The channel height for the foam-filled channel will be determined after the equal pressure drop and coolant flow rate are met.

For the foam-channel applications to be feasible in liquid-fueled rocket engines, the issue of pressure drop (rather than the pumping power) must be weighed with the heat transfer enhancement, because we can see that the penalty is severe from pressure losses. The heat transfer and pressure-drop experimental data obtained in our laboratory that are presented and discussed in the previous section are replotted with the heat transfer coefficient as a function of the pressure drop per unit length in Fig. 13. It provides a summary of the experimental data for both the copper and the nickel foams. The results are plotted based on heat transfer coefficient vs pressure drop per unit length. The highest Reynolds number exceeds 40,000. Both the copper and nickel foams show similar heat transfer and pressure-drop characteristics and magnitudes. The nickel-foam data exhibit scattering due to more rough surfaces and edges on the foam ligaments, because nickel is a harder material.

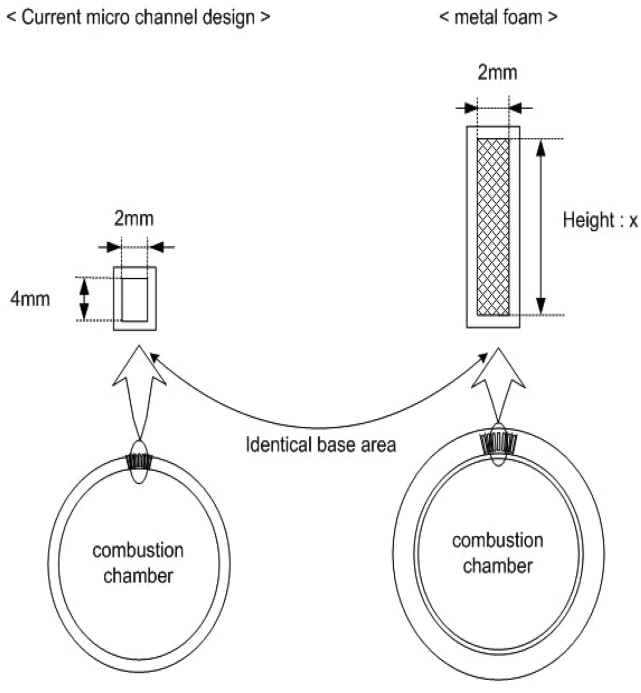

Fig. 12 Open microchannel model vs foam-filled channel model.

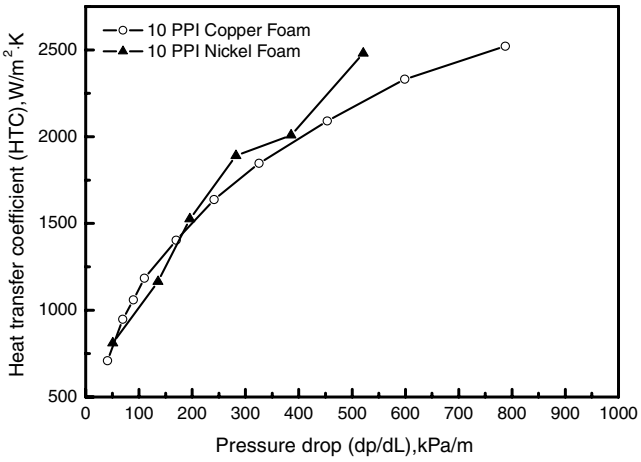

Fig. 13 Experimental data.

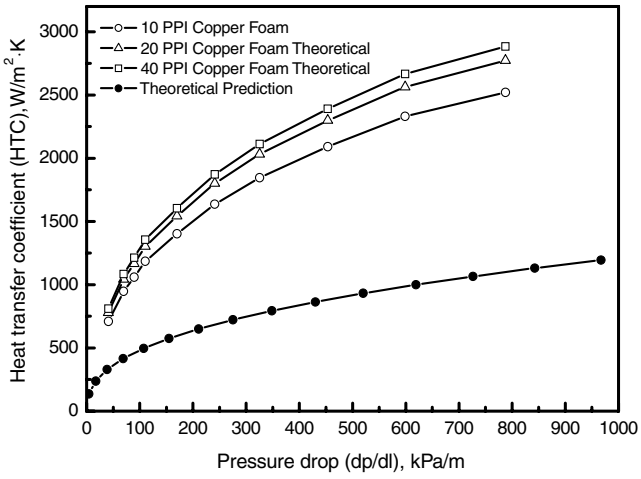

Fig. 14 Comparison between micro open channel and foam channel.

B. Comparison and Feasibility Study

Figure 14 shows a head-to-head comparison between the two models, as given in Fig. 12. The 10-PPI curve is generated from our experimental data, as given in Fig. 14. The 20- and 40-PPI curves were estimated by extrapolating the 10-PPI data using the correlations for heat transfer and pressure drop reported by Leong and Jin [8]. It is important to note that the proposed correlations [8] basically show that the heat transfer and pressure drop are functions of the pore size and are therefore independent of the length scale of the flow channel. Additionally, Lu et al. [19] demonstrated experimentally that pressure drop and heat transfer are primarily the same for pipes with diameters of 0.005 and 0.01 m.

For the micro-open-channel case, the pressure drop and heat transfer were estimated using correlations recommended by Incropera and DeWitt [20]. As shown in Fig. 14, the curves generally exhibit a slope under $Re = 10,000$ for laminar flow and then they flatten out somewhat for the turbulent flow. But it is noticeable that the microchannel curve flattens more than the foam-channel curve, probably due to different turbulent flow structures. Table 3 lists the percent of enhancement of the foam channel in heat transfer under an equal pressure drop and an equal mass flow rate using data taken from Fig. 14. The enhancement ranges from 105 to 150%. As already indicated, the enhancement increases with the pressure drop or Darcy velocity. Table 4 provides the required velocities in the two channels, respectively, for the same pressure drop. The results indicate that the foam channel should be 3 times larger than the micro open channel to maintain the same mass flow rate. Because both channels have the same base width, the height of the foam-filled channel should therefore be 3 times taller, which is 12 mm, to maintain equal mass flow rates with the microchannel.

VI. Conclusions

An experimental system was designed and constructed to investigate the heat transfer enhancement and the pressure drop in an annular channel filled with nickel or copper foams. The coolant was compressed air at 1378 kPa. Constant-heat-flux heaters placed inside the inner tube of the annulus were used to simulate the heat source. For the nickel-foam-filled annular channel, the heat transfer enhancement was found to be on the order of 20 times over the annular channel without porous insert for the same Darcy velocities. At equal pumping powers in the range of 10 to 100 W, the heat transfer enhancement of a metal-foam channel over an annular channel without porous insert is around 3 to 4 times.

In assessing the feasibility of applying the metal-foam-filled cooling channel for liquid-fueled rocket engines, we found that with the laboratory-scale and lower-speed airflow conditions, the foam-filled channel is capable of offering 105 to 150% improvement in heat transfer over a typical thrust-chamber microchannel under equal pressure drop and mass flow rate.

Table 3 Heat transfer enhancement at equal pressure drop

Pressure drop, psi/in.	Percent enhancement over microchannel for 10-PPI metal foam	Percent enhancement over microchannel for 20-PPI metal foam	Percent enhancement over microchannel for 40-PPI metal foam
1.0 (0.27 MPa/m)	136%	160%	170%
1.5 (0.41 MPa/m)	137%	160%	171%
2.0 (0.54 MPa/m)	137%	161%	172%
2.5 (0.68 MPa/m)	131%	154%	165%
2.75 (0.75 MPa/m)	130%	153%	164%

Table 4 Velocity ratio at equal pressure drop

Pressure drop, psi/in.	Velocity in copper foam, m/s	Velocity in microchannel, m/s	Velocity ratio
3.0 (0.81 MPa/m)	27.44	275	1:10.02
2.5 (0.68 MPa/m)	25.30	255	1:10.07
2.0 (0.54 MPa/m)	23.48	225	1:9.58
1.5 (0.41 MPa/m)	20.73	197	1:9.50
1.0 (0.27 MPa/m)	17.68	160	1:9.05
0.5 (0.14 MPa/m)	13.11	116	1:8.84
0.15 (0.04 MPa/m)	6.10	63	1:10.32

Acknowledgments

This work was performed with support from NASA Constellation University Institute Program (CUIP) under grant NCC3-994 with Claudia Meyer as the Program Manager. The support by the Andrew H. Hines, Jr. Progress Energy Endowment Fund is also acknowledged. Enthusiasm, encouragement, and advice provided to us by Bill Watkins of Pratt and Whitney, United Technologies, are greatly appreciated.

References

[1] Koh, J. C. Y., and Colony, R., "Analysis of Cooling Effectiveness for Porous Material; in a Coolant Passage," *Journal of Heat Transfer*, Vol. 96, No. 3, 1974, pp. 324–330.

[2] Koh, J. C. Y., and Stevens, R. L., "Enhancement of Cooling Effectiveness by Porous Materials in Coolant Passage," *Journal of Heat Transfer*, Vol. 97, No. 2, 1975, pp. 309–311.

[3] Hunt, M. L., and Tien, C. L., "Effects of Thermal Dispersion on Forced Convection Fibrous Media," *International Journal of Heat and Mass Transfer*, Vol. 31, No. 2, 1988, pp. 301–309.
doi:10.1016/0017-9310(88)90013-0

[4] Maiorov, V. A., Polyaev, V. M., Vasilev, L. L., and Kiselev, A. I., "Intensification of Convective Heat Exchange in Channels with a Porous High-Thermal-Conductivity Filler. Heat Exchange with Local Thermal Equilibrium Inside the Permeable Matrix," *Journal of Engineering Physics*, Vol. 47, No. 1, 1985, pp. 748–757.

[5] Bartlett, R. F., and Viskanta, R., "Enhancement of Forced Convection in an Asymmetrically Heated Duct Filled with High Thermal Conductivity Porous Media," *Journal of Enhanced Heat Transfer*, Vol. 6, No. 1, 1996, pp. 1–9.

[6] Kuzay, T. M., Collins J. T., and Koons, J., "Boiling Liquid Nitrogen Heat Transfer in Channels with Porous Copper Inserts," *International Journal of Heat and Mass Transfer*, Vol. 42, No. 7, 1999, pp. 1189–1204.
doi:10.1016/S0017-9310(98)00248-8

[7] Boomsma, K., Poulikakos, D., and Zwick, F., "Metal Foams as Compact High Performance Heat Exchangers," *Mechanics of Materials*, Vol. 35, No. 12, 2003, pp. 1161–1176.
doi:10.1016/j.mechmat.2003.02.001

[8] Leong, K. C., and Jin, L. W., "Effect of Oscillatory Frequency on Heat Transfer in Metal Foam Heat Sink of Various Pore Densities," *International Journal of Heat and Mass Transfer*, Vol. 49, Nos. 3–4, 2006, pp. 671–681.
doi:10.1016/j.ijheatmasstransfer.2005.08.015

[9] Kim, S. Y., Kang, B. H., and Kim, J. H., "Forced Convection from Aluminum Metal Foam Materials in an Asymmetrically Heated Channel," *International Journal of Heat and Mass Transfer*, Vol. 44, No. 7, 2001, pp. 1451–1454.
doi:10.1016/S0017-9310(00)00187-3

[10] Hwang, J. J., Hwang, G. J., Yeh, R. H., and Chao, C. H., "Measurement of Interstitial Convective Heat Transfer and Frictional Drag for Flow Across Metal Foams," *Journal of Heat Transfer*, Vol. 124, No. 1, 2002, pp. 120–129.
doi:10.1115/1.1416690

[11] Calmidi, V. V., and Mahajan, R. L., "Forced Convection in High Porosity Metal Foams," *Journal of Heat Transfer*, Vol. 122, No. 3, 2000, pp. 557–565.
doi:10.1115/1.1287793

[12] Lu, W., Zhao, C. Y., and Tassou, S. A., "Thermal Analysis on Metal-Foam Filled Heat Exchangers, Part 1 : Metal Foam Filled Pipes," *International Journal of Heat and Mass Transfer*, Vol. 49, Nos. 15–16, 2006, pp. 2751–2761.
doi:10.1016/j.ijheatmasstransfer.2005.12.012

[13] Lu, W., Zhao, C. Y., and Tassou, S. A., "Thermal Analysis on Metal-Foam Filled Heat Exchangers, Part 2 : Tube Heat Exchangers," *International Journal of Heat and Mass Transfer*, Vol. 49, 2006, pp. 2762–2770.
doi:10.1016/j.ijheatmasstransfer.2005.12.014

[14] Duklan, N., Quinone-Ramos, P. D., Cruz-Ruiz, E., Velez-Reyes, M., and Scott, E. P., "One-Dimensional Heat Transfer Analysis in Open-Cell 10-ppi Metal Foam," *International Journal of Heat and Mass Transfer*, Vol. 48, Nos. 25–26, 2005, pp. 5112–5120.
doi:10.1016/j.ijheatmasstransfer.2005.07.012

[15] Prandtl, L., *The Mechanics of Viscous Fluids*, Aerodynamic Theory, Vol. 3, Springer, Berlin, 1935.

[16] Gnielinski, V., "New Equations for Heat and Mass Transfer in Turbulent Pipe and Channel Flows," *International Chemical Engineering*, Vol. 16, No. 2, 1976, pp. 359–368.

[17] Sutton, G. P., and Biblarz, O., *Rocket Propulsion Elements*, 7th ed., Wiley-Interscience, New York, 2001.

[18] Wennerberg, J. C., Anderson, W. E., Haberlen, P. A., Jung, H., and Merkle, C. L., "Supercritical Flows in High Aspect Ratio Cooling Channels," 41st AIAA/ASME/SAE/ASEE Joint Propulsion Conference and Exhibit, Tucson, AZ, AIAA Paper 2005 4302, July 2005.

[19] Lu, W., Zhao, C. Y., and Tassou, S. A., "Thermal Analysis on Metal-Foam Filled Heat Exchangers Part 1 : Metal-Foam Filled Pipes," *International Journal of Heat and Mass Transfer*, Vol. 49, Nos. 5–6, 2006, pp. 986–997.

[20] Incropera, F., and DeWitt, D., *Fundamentals of Heat and Mass Transfer*, 5th ed., Wiley, New York, 2003.